# Spatial-temporal tensor completion methods with applications to space weather

Yang Chen
This talk is based on joint work with Hu Sun, Shasha Zou, Zuofeng Shang, Zihan Wang, Anthea Coster, Jingyang Li, Jiuqian Shang

Department of Statistics, University of Michigan


# Outline

1. Motivating Science Topic: Space Weather Monitoring
2. **Imputation**: Spatio-Temporal Matrix Completion Method (**VISTA**)
3. Data Product: Constructing A Space Weather Database with VISTA
4. **Completion**: FLOST

# Outline

# Motivating Science Topic: Space Weather Monitoring

Weather within our atmosphere: rain, snow, heat, and wind. Space weather: radio blackouts, solar radiation storms, and geomagnetic storms caused by disturbances from the Sun.

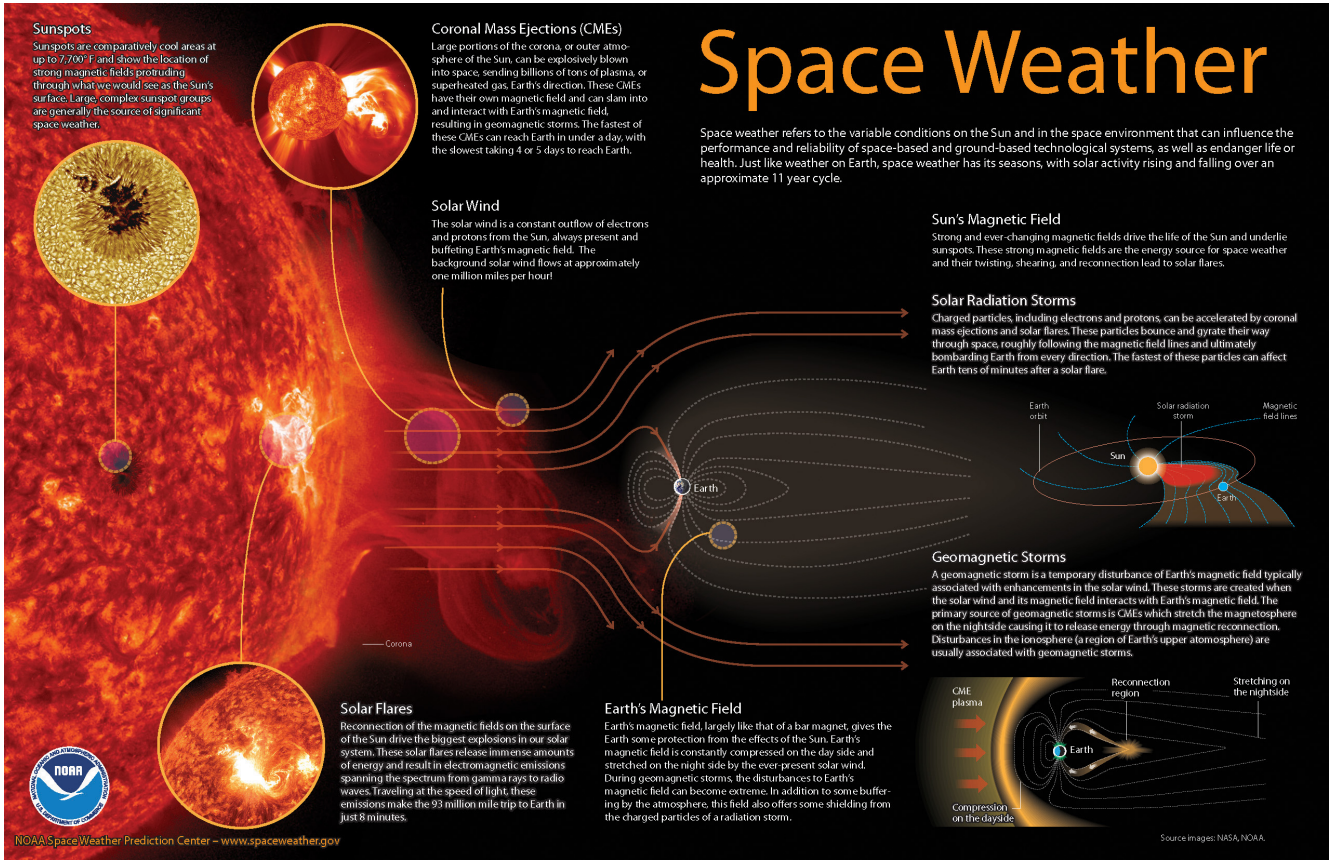


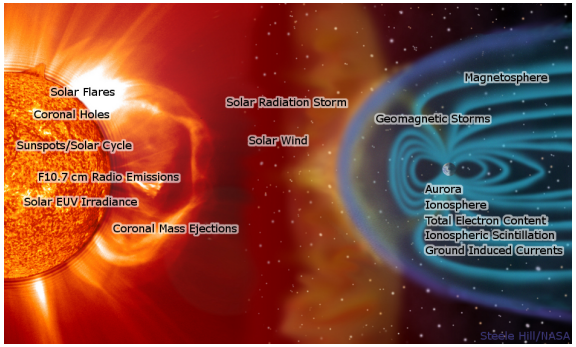


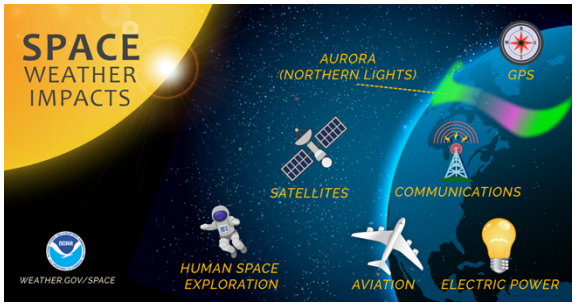


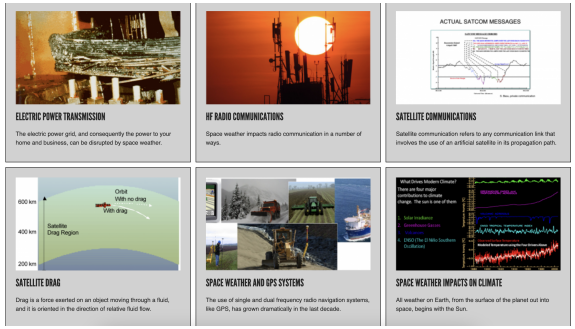

# Motivating Case in Space Weather: The TEC

Earth's Ionosphere: part of the upper atmosphere ionized by extreme ultraviolet (EUV) and x-ray solar radiation. Figures: Ionospheric effects on radio propagation and measurement of the total electron content (TEC).

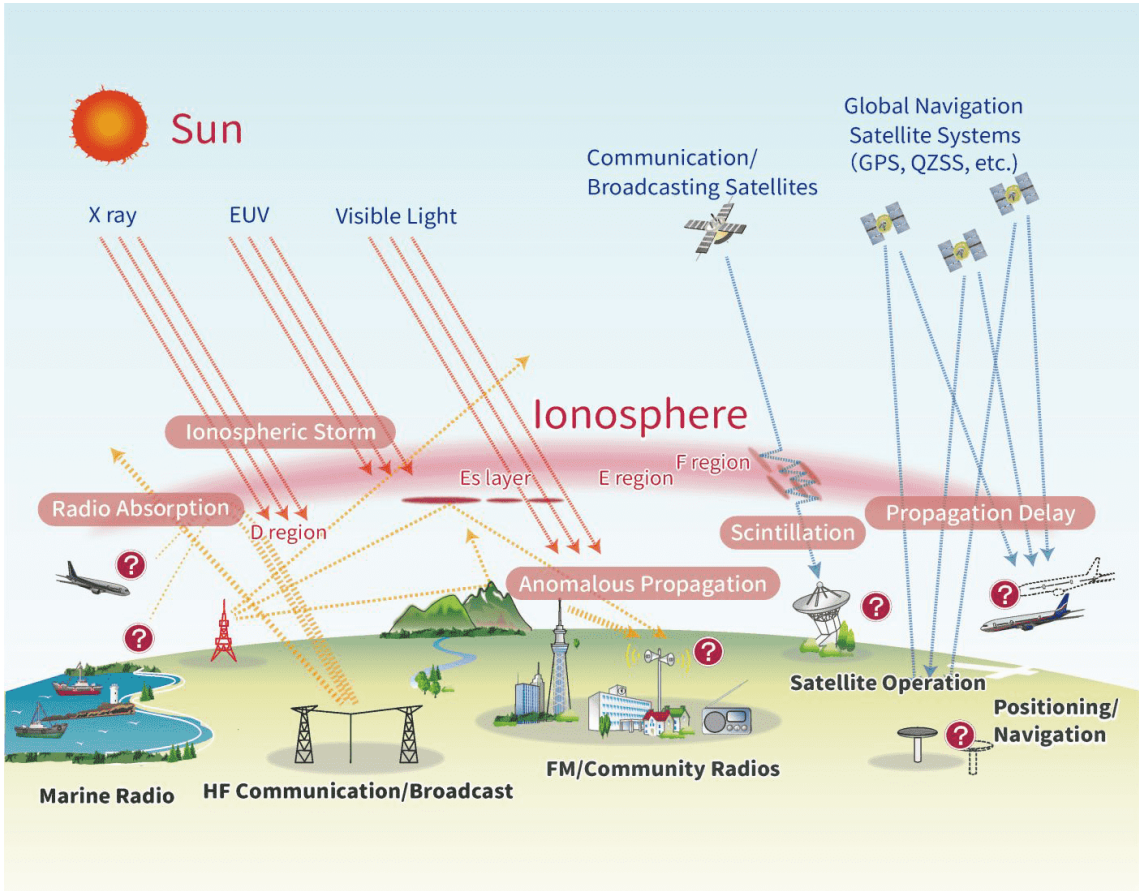


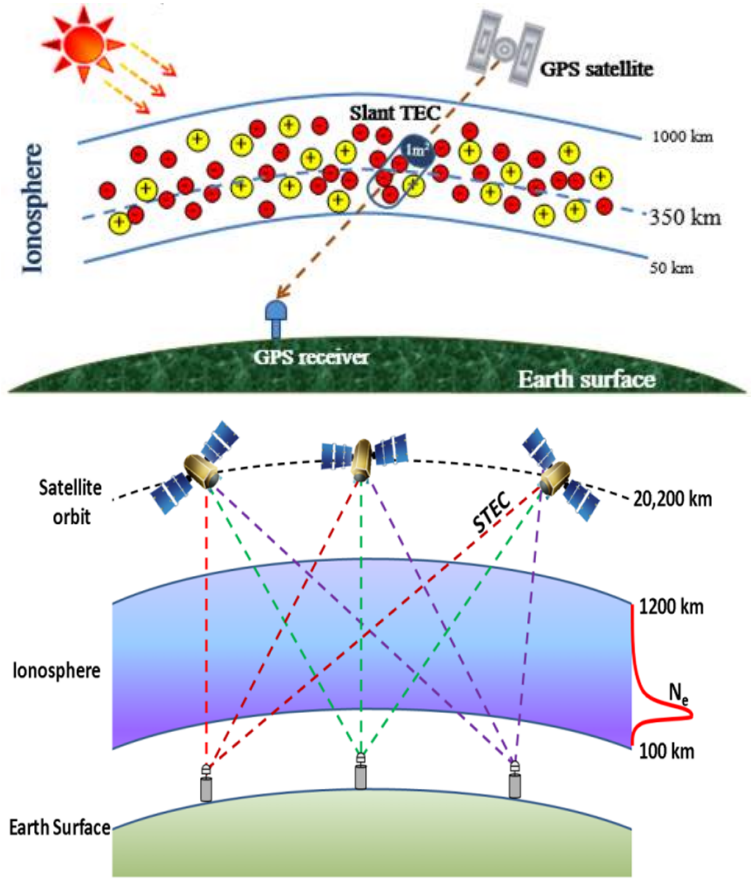

# Importance of Monitoring Total electron content (TEC)

- The change in the path and velocity of radio waves in the ionosphere greatly impacts the accuracy of satellite navigation systems such as GPS/GNSS.
- Neglecting changes in the ionospheric TEC can introduce tens of meters of error in the position calculations. The more electrons in the path of the radio wave, the more the radio signal will be affected.
- For ground-to-satellite communication and satellite navigation, TEC is a good parameter to monitor for possible space weather impacts.

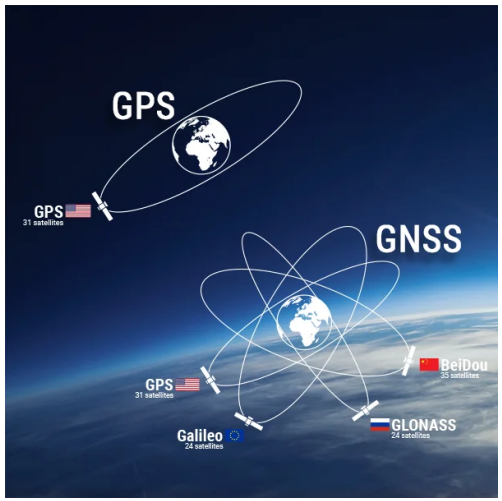


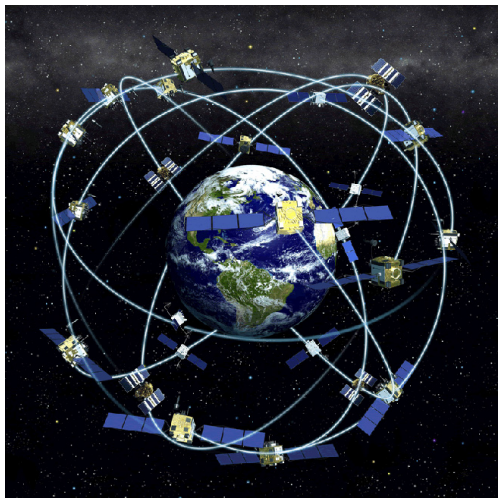

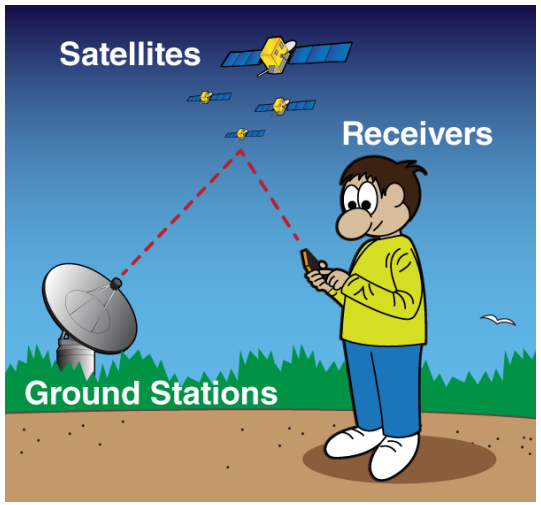

# Motivating Case in Space Weather: The TEC Data

Global **total electron content** (TEC) time series: TEC is an essential quantity for space weather monitoring but is sparsely observed, especially in the oceanic regions due to the lack of ground-based receivers.

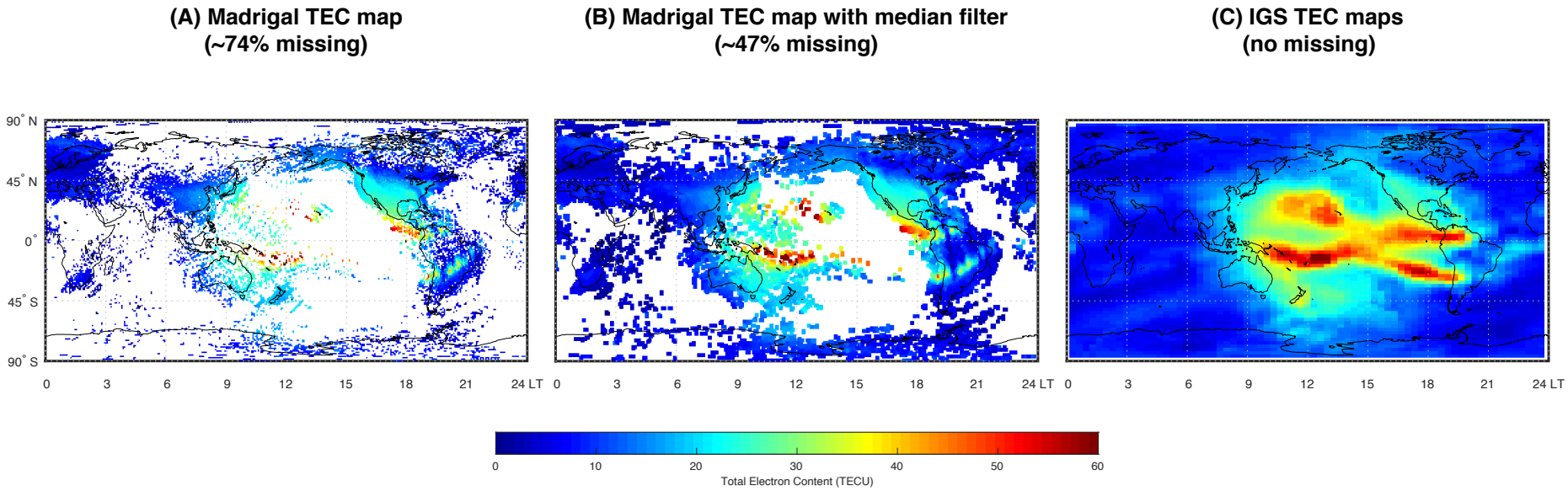


Figure 1.1: (A) Global Total Electron Content (TEC) Map, white pixels are missing data; (B) Median-Filtered TEC Map. (C) The popularly used imputation of the TEC in the geoscience community (spherical Harmonics) is typically overly smoothed.

# Statistical Problems with TEC Data

*Spatio-temporal tensor data* expressed as a 3-mode tensor data $\mathcal{X} \in \mathbb{R}^{m \times n \times T}$:

- $\mathcal{X}$ consists of a time series of spatial data. Let $\mathcal{X}_{::t} := \mathbf{X}_t \in \mathbb{R}^{m \times n}$.
- Each $\mathbf{X}_t$ is spatial data collected on an $m \times n$ grid, and is only *partially* observed. For $\mathbf{X}_t$, binary matrix $\mathbf{\Omega}_t$ denotes the missingness:

$$\mathbf{\Omega}_t(i,j) = \begin{cases} 1, & \text{if } \mathbf{X}_t(i,j) \text{ is observed,} \\ 0, & \text{if } \mathbf{X}_t(i,j) \text{ is missing.} \end{cases}$$

- Statistical questions:
  1. **Video Completion**: given the observations in $\mathbf{X}_1, \ldots, \mathbf{X}_T$ (indexed by $\mathbf{\Omega}_1, \ldots, \mathbf{\Omega}_T$), can we impute the missing values?
  2. **Map Prediction**: given the observations in $\mathbf{X}_1, \ldots, \mathbf{X}_{t-1}$, and other (global) vector time series predictors, can we predict $\mathbf{X}_t$?
  3. Proper uncertainty quantification for the two problems above.

# Outline

# Imputation Problem Formulated as Matrix Completion

## The Matrix Completion Problem

- Partially observed $m \times n$ matrix: $\mathbf{X}$.
- Binary indicator of observed entries: $\mathbf{\Omega}$.
- Projection operator: $\mathrm{P}_{\Omega}(\cdot)$, where

$$\mathrm{P}_{\Omega}(\mathbf{X}) = \begin{cases} \mathbf{X}(i,j) & \text{if } \mathbf{\Omega}(i,j) = 1 \\ 0 & \text{if } \mathbf{\Omega}(i,j) = 0 \end{cases}.$$

The matrix completion problem seeks a matrix $\widehat{\mathbf{X}} \in \mathbb{R}^{m \times n}$ such that:

$$\widehat{\mathbf{X}} = \underset{\mathrm{M} \in \mathbb{R}^{m \times n}}{\arg\min} \underbrace{\| \mathrm{P}_{\Omega} (\mathbf{X} - \mathbf{M}) \|_{\mathrm{F}}^2}_{\text{goodness-of-fit on the observed entries}} + \overbrace{\lambda g(\mathbf{M})}^{\text{penalty of matrix complexity}}.$$

# Matrix Completion for Spatial Data: Does it Work?

The soft-Impute algorithm in [Hastie et al., 2015] gives:

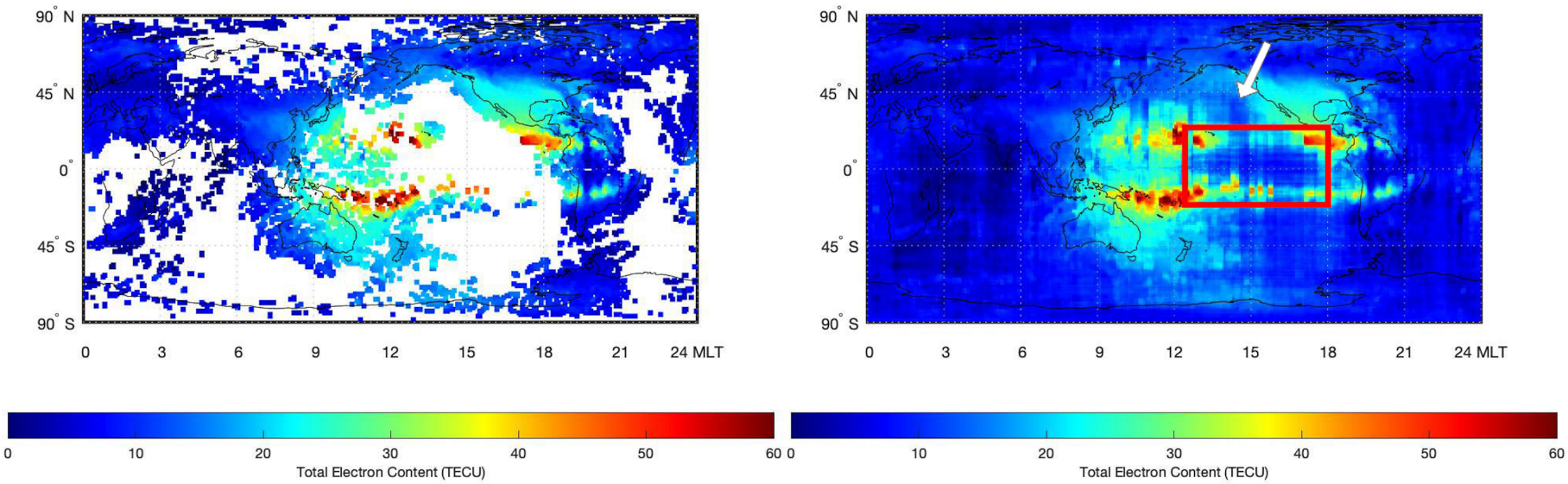


Figure 2.1: Left: Source matrix. Right: Imputed matrix based on Soft-Impute.

The result is *problematic scientifically* because the completed maps are:

- not spatially smooth (the blue bands); and
- not informative when missingness are spatially clustered (the red box).

# Alternative: Kernel Smoothing for Matrix Completion

Recall the matrix completion problem:

$$\widehat{\mathbf{X}} = \underset{\mathrm{M}\in\mathbb{R}^{m\times n}}{\arg\min} \|\mathrm{P}_{\Omega}\left(\mathbf{X}-\mathbf{M}\right)\|_{\mathrm{F}}^{2} + \lambda g(\mathbf{M}).$$

In a kernel smoothing method, one assumes that $\mathbf{M}$ is a discrete evaluation of an unknown function $f$ on the matrix grid. Specifically,

$$\mathbf{M}(i,j) = f(s_{ij})$$

where $s_{ij} \in \mathbb{R}^2$ is the spatial location of the $(i,j)$-th entry. And $g(\mathbf{M})$ is a penalty on the functional parameter $g$, e.g., the functional norm in a Hilbert space.

Widely adopted kernel in space weather: spherical Harmonics.

# Alternative: Kernel Smoothing for Matrix Completion

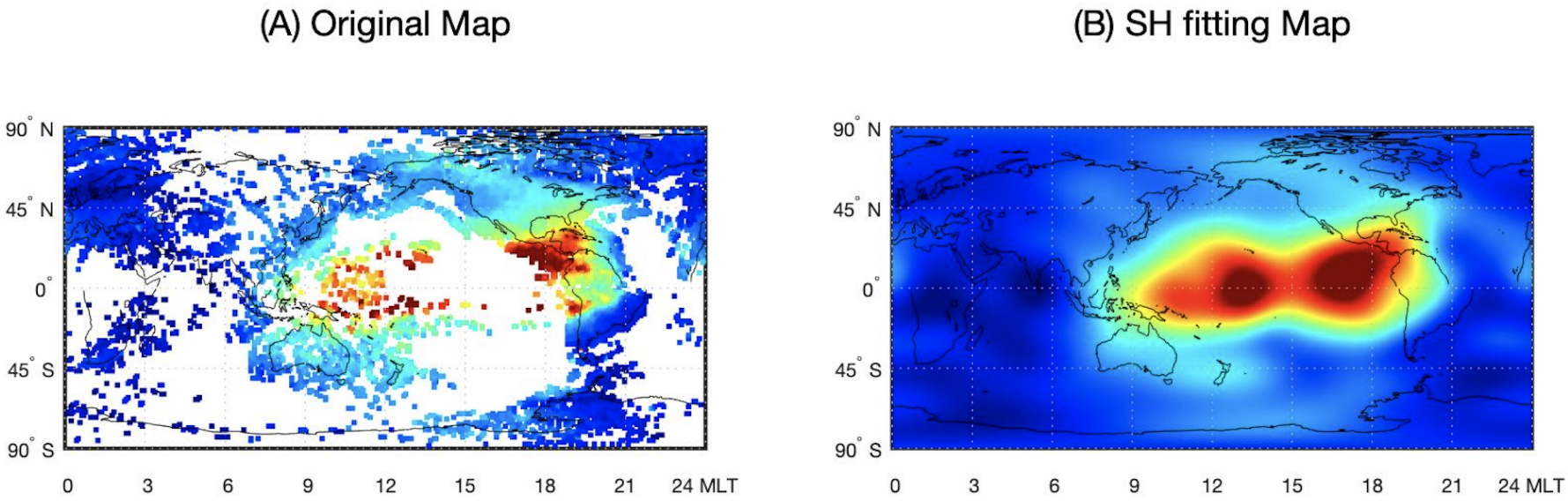


Figure 2.2: Example of Spherical Harmonics Kernel Smoothing

The result from Spherical Harmonics fitting is:

- poorly fitted over the observed entries; and
- overly smooth locally but capture the global trend.

# Proposed Method: The VISTA Approach

We aim to develop a method that:

- simultaneously imputes all $\mathbf{X}_1, \ldots, \mathbf{X}_T$;
- fits well on the scattered missing entries in $\mathbf{X}_1, \ldots, \mathbf{X}_T$, and
- fits well over the large-patch missingness.

A novel tensor completion approach, named **VISTA**, bridges

- Soft-Impute ALS: low-rank matrix completion method, and
- Spherical Harmonics: kernel smoothing method, while
- accounting for temporal continuity & temporally varying missingness.

# Proposed Method: The VISTA Approach

## VISTA Video Imputation Method

We impute $\mathcal{X} \in \mathbb{R}^{m \times n \times T}$ by finding the minimizer of:

$$\min_{\mathrm{A}_t \in \mathbb{R}^{m \times r}, \mathrm{B}_t \in \mathbb{R}^{n \times r}, \forall t \in [T]} \frac{1}{2} \sum_{t=1}^{T} \| \mathrm{P}_{\Omega_t} \left( \mathbf{X}_t - \mathbf{A}_t \mathbf{B}_t^\top \right) \|_{\mathrm{F}}^2 + g_{\boldsymbol{\lambda}}(\mathbf{A}_1, \ldots, \mathbf{A}_T, \mathbf{B}_1, \ldots, \mathbf{B}_T)$$

where $g_{\boldsymbol{\lambda}}(\cdot)$ has the following three terms:

- $\frac{\lambda_1}{2} \sum_{t=1}^{T} \left( \|\mathbf{A}_t\|_{\mathrm{F}}^2 + \|\mathbf{B}_t\|_{\mathrm{F}}^2 \right)$: the **S**oft-impute penalty;
- $\frac{\lambda_2}{2} \sum_{t=2}^{T} \|\mathbf{A}_t \mathbf{B}_t^\top - \mathbf{A}_{t-1} \mathbf{B}_{t-1}^\top\|_{\mathrm{F}}^2$: the **T**emporal smoothness penalty;
- $\frac{\lambda_3}{2} \left\| \mathbf{Y}_t - \mathbf{A}_t \mathbf{B}_t^\top \right\|_{\mathrm{F}}^2$: the **A**uxiliary algorithm (data) penalty.

We coined the term VISTA since the method is a **V**ideo **I**mputation method with **S**oft-impute, **T**emporal-smoothing and **A**uxiliary data.

# Simulation Experiment - Design

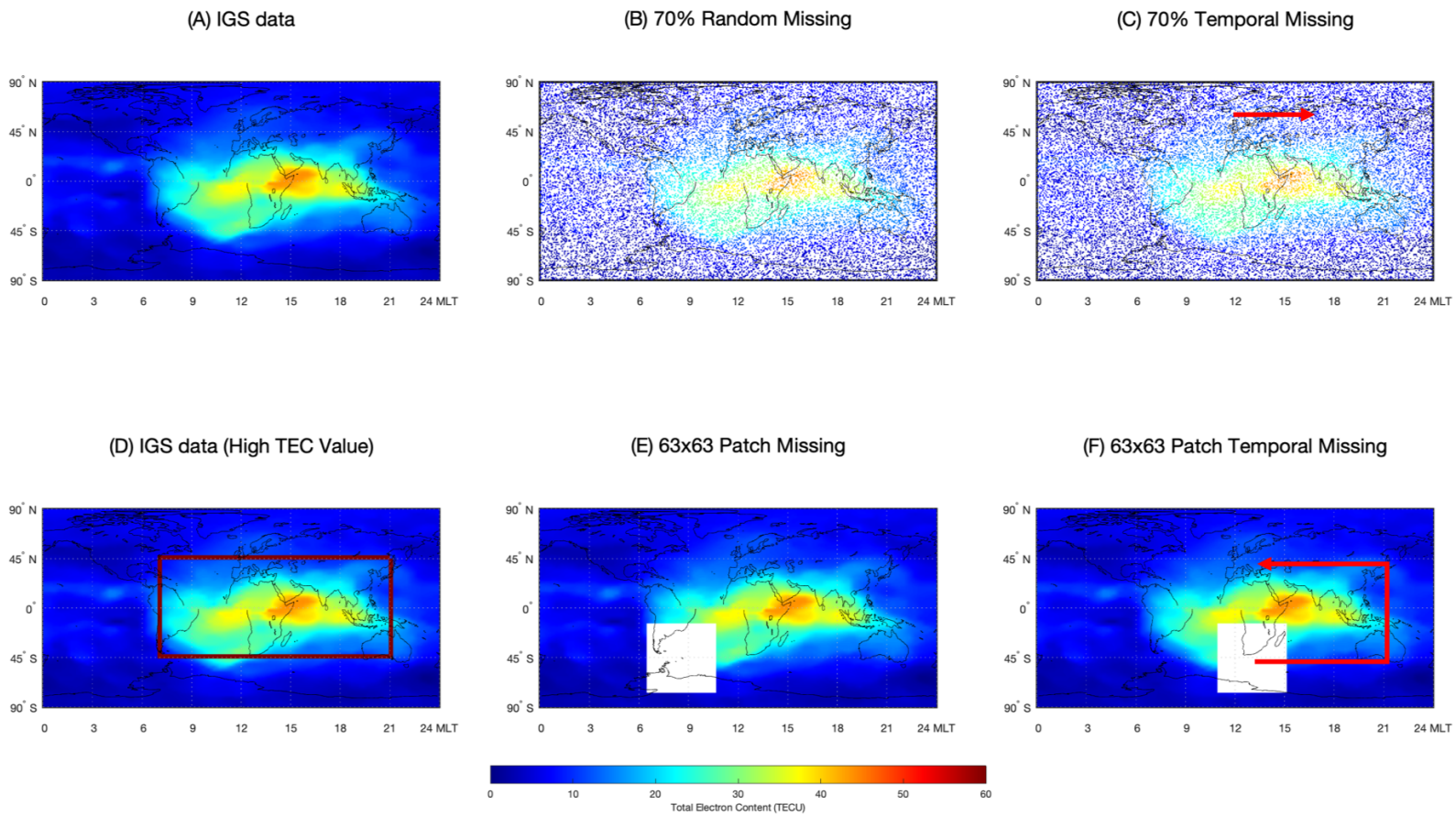


Figure 2.3: (A) Ground Truth; (B) random+non-temporal+70%; (C) random+temporal+70%; (E) patch+non-temporal+$63 \times 63$; (F) patch+temporal+$63 \times 63$.

# Simulation Experiment - Result

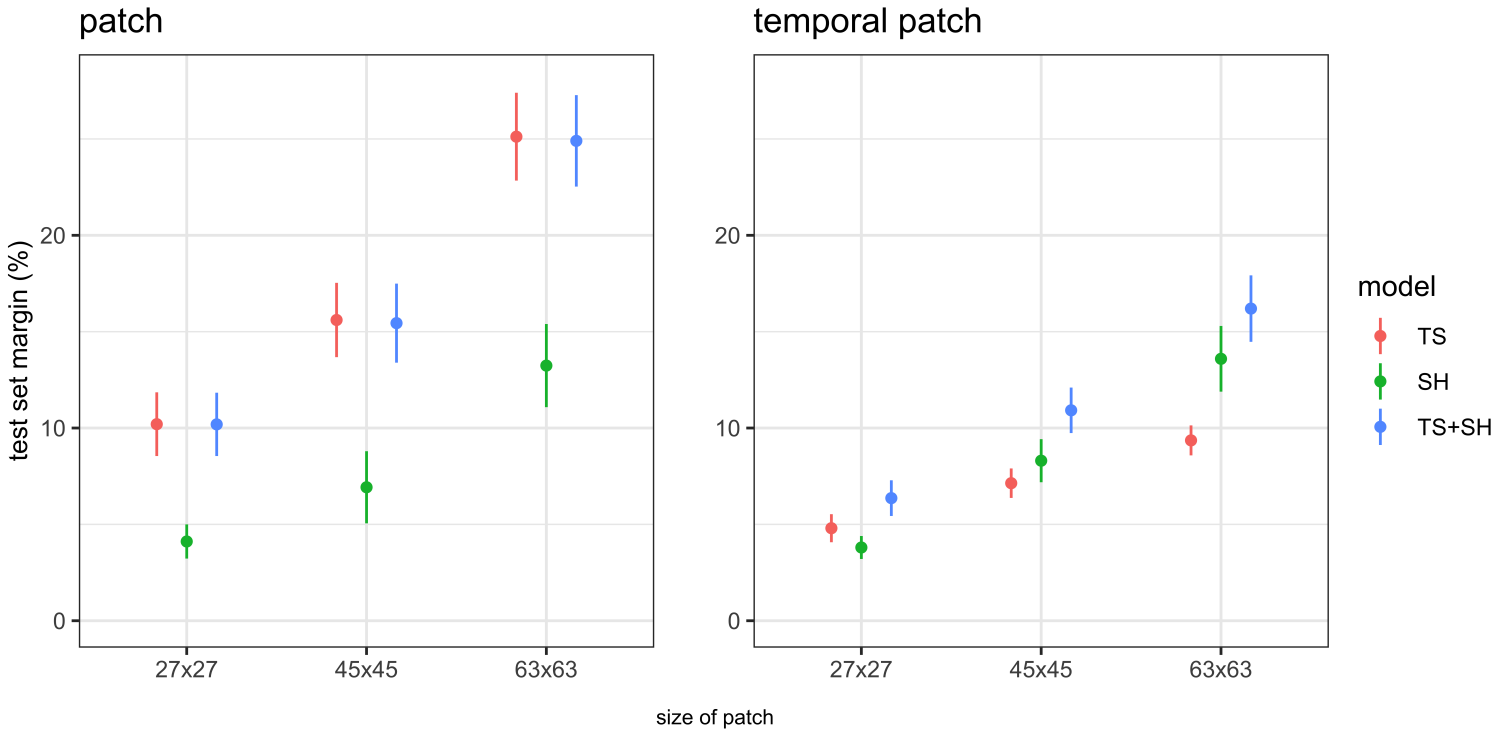


Figure 2.5: Patch+non-temporal missing (left) and Patch+temporal patch missing (right) results. The scatter points show the average test set RSE margin over the baseline softImpute method, **positive means performance better than softImpute**. Error bar gives the 95% confidence interval.

# Real Data Implementation - Result

Applying the VISTA method to the high-resolution global TEC data:

| Storm Day | | | | |
|---|---|---|---|---|
| Model | test RSE | test MSE | # matrices better than softImpute | # matrices worse than Full model |
| softImpute ($\lambda_1 = 0.9$) | 10.895% | 2.675 | / | 285 (98.96%) |
| TS ($\lambda_1 = 0.9, \lambda_2 = 0.2$) | 9.643% | 2.106 | 284 (98.62%) | 267 (92.71%) |
| SH ($\lambda_1 = 0.9, \lambda_3 = 0.021$) | 9.936% | 2.227 | 287 (99.65%) | 274 (95.14%) |
| Full ($\lambda_1 = 0.9, \lambda_2 = 0.2, \lambda_3 = 0.021$) | 9.357% | 1.983 | 285 (98.96%) | / |
| Directly use Spherical Harmonics | 17.354% | 6.720 | 0 (0%) | 288 (100%) |
| **Non-Storm Day** | | | | |
| Model | test RSE | test MSE | # matrices better than softImpute | # matrices worse than Full model |
| softImpute ($\lambda_1 = 0.9$) | 10.424% | 1.324 | / | 283 (98.26%) |
| TS ($\lambda_1 = 0.9, \lambda_2 = 0.31$) | 8.880% | 0.958 | 281 (97.57%) | 235 (81.60%) |
| SH ($\lambda_1 = 0.9, \lambda_3 = 0.03$) | 9.231% | 1.032 | 287 (99.65%) | 278 (96.53%) |
| Full ($\lambda_1 = 0.9, \lambda_2 = 0.31, \lambda_3 = 0.03$) | 8.592% | 0.895 | 283 (98.26%) | / |
| Directly use Spherical Harmonics | 15.732% | 2.893 | 0 (0%) | 288 (100%) |

Table 1: Empirical study results from the madrigal database.

Figure 2.6: Storm day is Sept-08, 2017 and non-storm day is Sept-03, 2017.

# Summary

In this project, we:

- propose a spatiotemporal video completion method **VISTA** by modifying classical matrix completion method with:
  1. temporal variation regularization;
  2. regularization based on an auxiliary data/algorithm (kernel smoothing)
- establish the convergence guarantee of the algorithm;
- validate the method with extensive simulation & real data experiments.

**Our paper**: Sun, H., Hua, Z., Ren, J., Zou, S., Sun, Y., & **Chen, Y.** (2022). Matrix Completion Methods for the Total Electron Content Video Reconstruction. *The Annals of Applied Statistics*, 16(3), 1333-1358.

# Outline

# The VISTA TEC Database


Figure 3.1: The VISTA TEC Open Source Database [link].

# The VISTA TEC Workflow

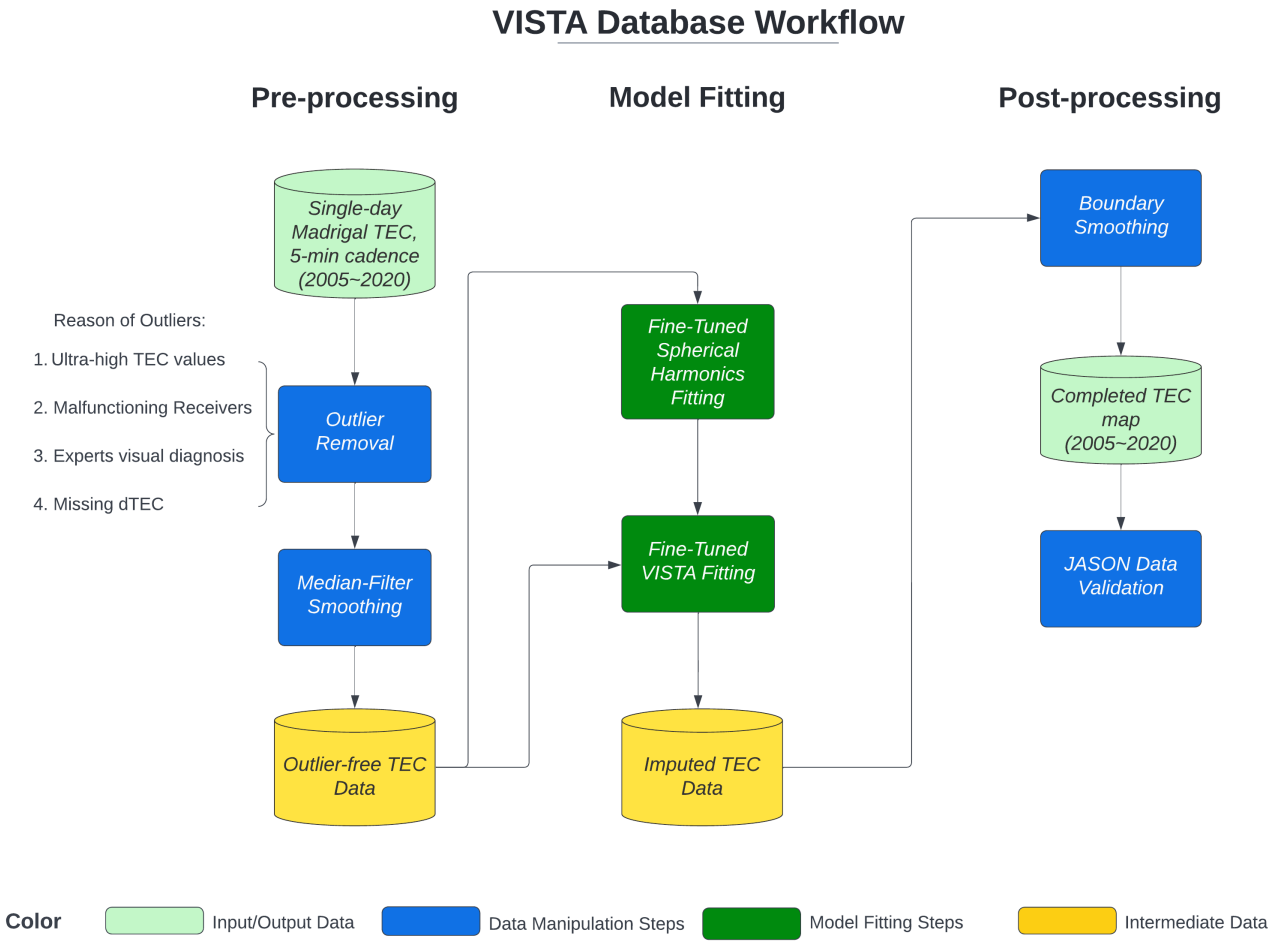


Figure 3.2: The Database Generating Workflow. Image source: Sun et al. [2023].

# Sample of the VISTA TEC Database

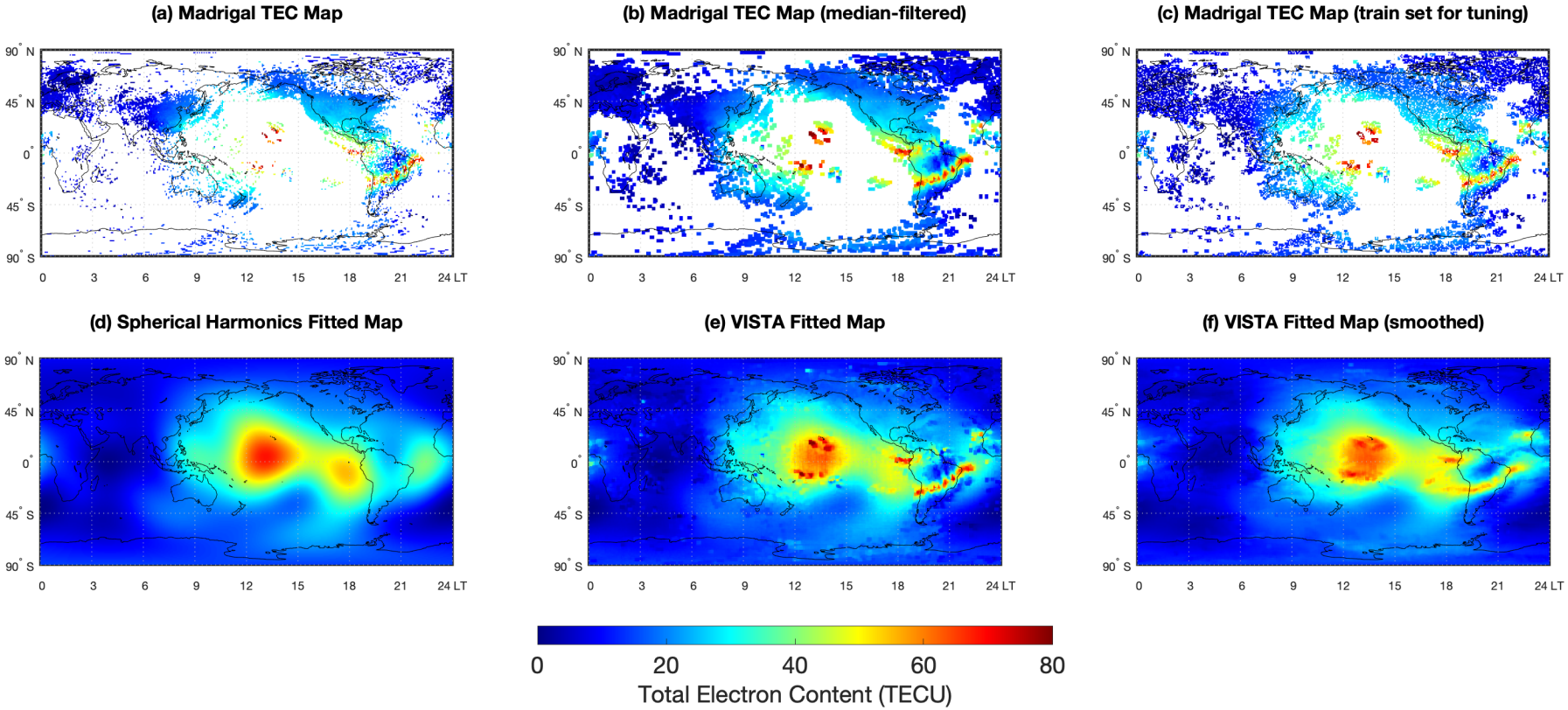


Figure 3.3: TEC maps throughout the workflow. Image source: Sun et al. [2023].

# Summary

In this project, we:

- create a 16-year spatiotemporal database for the global TEC with VISTA;
- achieve higher imputation accuracy and higher spatiotemporal resolution as compared to previous open source databases;
- validate the imputed entries in the VISTA TEC maps with an independent data source.

**Our paper**: Sun, H., **Chen, Y.**, Zou, S., Ren, J., Chang, Y., Wang, Z., & Coster, A. (2023). Complete Global Total Electron Content Map Dataset based on a Video Imputation Algorithm VISTA. *Scientific Data*, 10(1), 236.

# Outline

# Motivation

- Restating the TEC Completion problem as a tensor completion problem: $\mathcal{T} = [\mathbf{X}_1, \ldots, \mathbf{X}_T] \in \mathbb{R}^{M \times N \times T}$ with missingness given by $\Omega = \{(i, j, k), \omega_{ijk} = 1\}$, where $\omega_{ijk} \sim \text{Bernoulli}(p)$.

- Existing approach: low-rank structures given by CP Jain and Oh [2014]; Cai et al. [2022a], Tucker Xia and Yuan [2019]; Xia et al. [2021]; Li et al. [2023], Tensor-Train (TT) Cai et al. [2022c,b], and tubal-rank Zhang and Aeron [2016]; Liu et al. [2019]; Jiang and Ng [2019]; Song et al. [2023].

- Unique challenge:

  - stable/slow-varying TEC for many regions

  - rapid fluctuations for certain regions (geomagnetic storm)

# Definition

## Definition (Fourier Low-rank and Sparse Tensor)

We say a tensor $\mathcal{T} \in \mathbb{R}^{M\times N\times T}$ is $(\mathbf{r}, K, s)$-FLOST for $\mathbf{r} = (r_1, \cdots, r_K)$, if

$$\text{rank}(\mathcal{T} \times_3 \mathbf{f}_l^\top) \le r_l,\ l = 1, \cdots, K, \quad \|\mathcal{T} \times_3 \mathbf{F}_1^\top\|_0 \le s,$$

where $\mathbf{F}_1 = [\mathbf{f}_{K+1}, \cdots, \mathbf{f}_{\lceil \frac{T+1}{2} \rceil}]$ and $K \le \lceil \frac{T+1}{2} \rceil$.

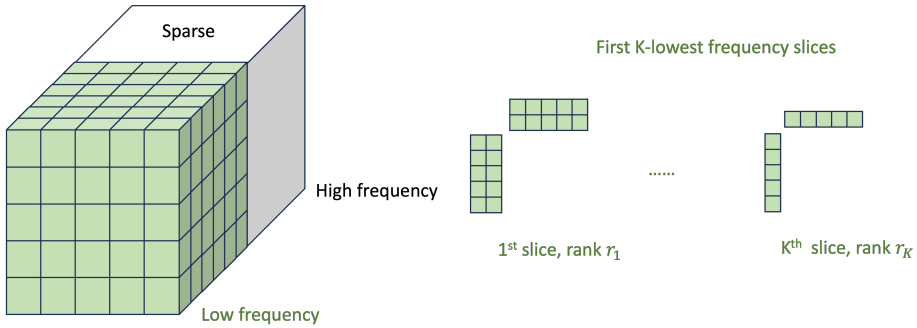


Figure 4.1: Structure of FLOST in the frequency domain.

Here, $\mathcal{T} \times_3 \mathbf{f}_l^\top$ extracts the $l$-th frontal slice of the tensor in the frequency domain, and $\mathcal{T} \times_3 \mathbf{F}_1^\top$ corresponds to the collection of high-frequency slices.

# Model and Loss

Let $\mathcal{T}_0 \in \mathbb{R}^{M\times N\times T}$ be a tensor that is $(\mathbf{r}, K, s)$-FLOST. We can obtain a collection of partially observed and noisy entries where the sampling indicator $\omega_{ijt} = 1$:

$$\mathcal{Y}_{ijt} = [\mathcal{T}_0]_{ijt} + \mathcal{E}_{ijt}.$$

Here $\mathcal{E}$ represents the random noise independent of $\{\omega_{ijt}\}_{ijt}$. We propose:

$$\hat{\mathcal{T}} := \arg\min_{\mathcal{T}\in\mathbb{R}^{M\times N\times T}} \frac{1}{2}\|\mathcal{T} - p^{-1}\mathcal{P}_\Omega(\mathcal{Y})\|_{\mathrm{F}}^2 + \sum_{l=1}^{K} \lambda_{1,l}\|\mathcal{T}\times_3 \mathbf{f}_l^\top\|_* + \lambda_2\|\mathcal{T}\times_3 \mathbf{F}_1^\top\|_{\ell_1}. \tag{1}$$

Here the nuclear norm and $\ell_1$ norm are the regularizations for the low-rank and sparse structures, respectively.

# Computation

**Parallel Implementation:**

Since $\|\mathcal{T} - p^{-1}\mathcal{P}_\Omega(\mathcal{Y})\|_{\mathrm{F}}^2 = \sum_{t=1}^{T} \|\left(\mathcal{T} - p^{-1}\mathcal{P}_\Omega(\mathcal{Y})\right) \times_3 \mathbf{f}_l^\top\|_{\mathrm{F}}^2$, the optimization problem in (1) can be equivalently written as $K+1$ independent problems in the Fourier domain:

$$\hat{\mathbf{T}}_l = \arg\min_{\mathbf{T}} \frac{1}{2}\|\mathbf{T} - p^{-1}\mathcal{P}_\Omega(\mathcal{Y}) \times_3 \mathbf{f}_l^\top\|_{\mathrm{F}}^2 + \lambda_{1,l}\|\mathbf{T}_l\|_*, \quad l = 1, \cdots, K \tag{2a}$$

$$\hat{\mathcal{T}}_1 = \arg\min_{\mathcal{T}} \frac{1}{2}\|\mathcal{T} - p^{-1}\mathcal{P}_\Omega(\mathcal{Y}) \times_3 \mathbf{F}_1^\top\|_{\mathrm{F}}^2 + \lambda_2\|\mathcal{T}\|_{\ell_1}. \tag{2b}$$

Once we obtain $\hat{\mathbf{T}}_l, \hat{\mathcal{T}}_1$, we first concatenate these matrices/tensor, then apply the inverse Fourier transform to recover the estimator for $\mathcal{T}_0$.

# Theoretical Guarantee

## Corollary

*Assume the noise $\mathcal{E}_{ijt}$ are independently distributed centered sub-Gaussian random variables with proxy variance $\sigma^2$, and $\max_{ijt} |[\mathcal{T}_0]_{ijt}| \leq \gamma$. Choose*

$$\lambda_{1,l} \geq C_1(\sigma \vee \gamma)\left(\frac{\sqrt{(N \vee M)\log(M \vee N)}}{\sqrt{p}} + \frac{\sqrt{\log^3(M \vee N)}}{p\sqrt{T}}\right),$$

$$\lambda_2 \geq C_2(\sigma \vee \gamma)\left(\frac{\sqrt{\log(M \vee N \vee T)}}{\sqrt{p}} + \frac{\log(M \vee N \vee T)}{\sqrt{T}p}\right).$$

*Assume* $n \geq \max\left\{(M \wedge N), \min\left\{(M \wedge N)\frac{s}{\sum_l r_l}, MN\right\}\right\}$, *then*

$$\frac{1}{MNT}\|\hat{\mathcal{T}} - \mathcal{T}_0\|_{\mathrm{F}}^2 \leq \tilde{C}\frac{\sum_{l=1}^K (M \vee N)r_l + s}{n}(\sigma \vee \gamma)^2$$

*holds with probability exceeding* $1 - 2(M \vee N \vee T)^{-10}$.

# Numerical Performance

| Method | $T = 100$ | | $T = 500$ | | $T = 1000$ | |
|---|---|---|---|---|---|---|
| | Test RMSE | Time | Test RMSE | Time | Test RMSE | Time |
| FLoST | 0.5183 ± 0.0123 | 0.06 ± 0.00 | 0.5216 ± 0.0132 | 0.31 ± 0.02 | 0.5198 ± 0.0147 | 0.69 ± 0.05 |
| Ablation | 0.5318 ± 0.0004 | 0.16 ± 0.01 | 0.5298 ± 0.0002 | 0.89 ± 0.08 | 0.5292 ± 0.0001 | 2.03 ± 0.16 |
| RCGD | 0.5785 ± 0.0005 | 0.47 ± 0.01 | 0.5753 ± 0.0002 | 2.81 ± 0.18 | 0.5743 ± 0.0002 | 6.59 ± 0.47 |
| Alt-Min-LS | 0.5423 ± 0.0006 | 8.88 ± 0.10 | 0.5406 ± 0.0003 | 47.76 ± 2.85 | 0.5399 ± 0.0002 | 95.24 ± 4.17 |
| LRTC-TNN | 0.5591 ± 0.0005 | 9.91 ± 0.52 | 0.5543 ± 0.0002 | 53.14 ± 4.84 | 0.5522 ± 0.0002 | 121.33 ± 10.52 |
| PRGD | 0.5496 ± 0.0004 | 6.18 ± 0.36 | 0.5475 ± 0.0002 | 33.15 ± 1.65 | 0.5469 ± 0.0001 | 67.37 ± 4.83 |

Table 1: Abalation: FLoST with no sparsity. LRTC-TNN [Lu et al., 2019], Alt-Min-LS [Liu et al., 2019] PRGD [Zhang et al., 2025].

# Conclusions

- VISTA TEC Database construction [Sun et al., 2022, 2023].
- FLoST Tensor Completion Algorithm [Li et al., 2025].
- Tensor completion with uncertainty quantification (UQ):
  - Conformalized tensor completion [Sun and Chen, 2024];
  - UQ for low-tubal rank tensor completion [Shang et al., 2026].
- Video/tensor prediction [Wu et al., 2026; Sun et al., 2024].
- Check out our newly developed spaceweatherlab.org

# References I

C. Cai, G. Li, H. V. Poor, and Y. Chen. Nonconvex low-rank tensor completion from noisy data. *Operations Research*, 70(2):1219–1237, 2022a.

J.-F. Cai, W. Huang, H. Wang, and K. Wei. Tensor completion via tensor train based low-rank quotient geometry under a preconditioned metric. *arXiv preprint arXiv:2209.04786*, 2022b.

J.-F. Cai, J. Li, and D. Xia. Provable tensor-train format tensor completion by riemannian optimization. *Journal of Machine Learning Research*, 23(123): 1–77, 2022c.

T. Hastie, R. Mazumder, J. D. Lee, and R. Zadeh. Matrix completion and low-rank svd via fast alternating least squares. *The Journal of Machine Learning Research*, 16(1):3367–3402, 2015.

P. Jain and S. Oh. Provable tensor factorization with missing data. *Advances in Neural Information Processing Systems*, 27, 2014.

Q. Jiang and M. Ng. Robust low-tubal-rank tensor completion via convex optimization. In *IJCAI*, pages 2649–2655, 2019.

# References II

J. Li, J.-F. Cai, Y. Chen, and D. Xia. Online tensor learning: Computational and statistical trade-offs, adaptivity and optimal regret. *arXiv preprint arXiv:2306.03372*, 2023.

J. Li, J. Shang, and Y. Chen. Fourier low-rank and sparse tensor for efficient tensor completion. *arXiv preprint arXiv:2505.11261*, 2025.

X.-Y. Liu, S. Aeron, V. Aggarwal, and X. Wang. Low-tubal-rank tensor completion using alternating minimization. *IEEE Transactions on Information Theory*, 66(3):1714–1737, 2019.

C. Lu, X. Peng, and Y. Wei. Low-rank tensor completion with a new tensor nuclear norm induced by invertible linear transforms. In *Proceedings of the IEEE/CVF conference on computer vision and pattern recognition*, pages 5996–6004, 2019.

J. Shang, J. Li, and Y. Chen. Uncertainty quantification for noisy low-tubal-rank tensor completion. *arXiv preprint arXiv:2604.10353*, 2026.

# References III

G.-J. Song, X.-Z. Wang, and M. K. Ng. Riemannian conjugate gradient descent method for fixed multi rank third-order tensor completion. *Journal of Computational and Applied Mathematics*, 421:114866, 2023.

H. Sun and Y. Chen. Conformalized tensor completion with riemannian optimization. *arXiv preprint arXiv:2405.00581*, 2024.

H. Sun, Z. Hua, J. Ren, S. Zou, Y. Sun, and Y. Chen. Matrix completion methods for the total electron content video reconstruction. *The Annals of Applied Statistics*, 16(3):1333–1358, 2022.

H. Sun, Y. Chen, S. Zou, J. Ren, Y. Chang, Z. Wang, and A. Coster. Complete global total electron content map dataset based on a video imputation algorithm vista. *Scientific Data*, 10(1):236, 2023.

H. Sun, Z. Shang, and Y. Chen. Matrix autoregressive model with vector time series covariates for spatio-temporal data. *arXiv preprint arXiv:2305.15671*, 2024.

# References IV

D. Wu, K. Jin, and Y. Chen. Tensortree regression with additional boosting for tensor prediction with auxiliary covariates, 2026.

D. Xia and M. Yuan. On polynomial time methods for exact low-rank tensor completion. *Foundations of Computational Mathematics*, 19(6):1265–1313, 2019.

D. Xia, M. Yuan, and C.-H. Zhang. Statistically optimal and computationally efficient low rank tensor completion from noisy entries. *The Annals of Statistics*, 49(1), 2021.

Y. Zhang, F. Bian, X. Zhang, and J.-F. Cai. Preconditioned riemannian gradient descent algorithm for low-multilinear-rank tensor completion. In *Forty-second International Conference on Machine Learning*, 2025.

Z. Zhang and S. Aeron. Exact tensor completion using t-svd. *IEEE Transactions on Signal Processing*, 65(6):1511–1526, 2016.